SAND2008-3541C

EFFECT OF HYBRIDIZATION ON COMPOSITE IMPACT RESISTANCE

E. Askari, K. Nelson, O. Weckner, J. Xu
The Boeing Company
Seattle, Washington, USA

S. A. Silling
Sandia National Laboratories
Albuquerque, New Mexico, USA

ABSTRACT

The impact of hail against a toughened-epoxy, intermediate-modulus, carbon-fiber composite is investigated experimentally and analytically. The effect of introducing ply-level hybridization by substituting up to 20% of the plies with glass-reinforced plies is considered. It is found that delamination can in many cases be reduced by this hybridization, but the benefits are dependent on the impact energy and the test conditions. A computational model based on the peridynamic theory of solid mechanics is used to understand the benefits and trade-offs in hybridization.

KEY WORDS: Impact Damage/Resistance/Behavior, Modeling Methodology, Hybrid Materials/Structures

1. INTRODUCTION

As a way to reduce the weight of graphite-epoxy composite laminates while preserving their structural properties, especially impact resistance, it has been proposed to replace a fraction of the graphite with glass or other fiber material. The resulting laminate, with multiple fiber types, is called a *hybrid* composite. The concept of a hybrid composite was being explored as early as the 1970's, for example by Adams and Miller (1975); Beaumont, Riewald, and Zweben (1975); and Dorey, Sidey, and Hutchings (1978). Interest has continued to the present, including Lee, Kang and Park (1997); Naik et al. (2001); and Park and Jang (2001).

One approach to hybridization is to replace only part of the fibers within individual plies, and the resulting laminate is called a *tow-level* hybrid. However, the present paper is concerned with replacing all the fibers within certain plies by glass fibers, resulting in a *ply-level* hybrid. Ply-level hybridization introduces several new variables into the design of a laminate, in addition to the choice of what type of glass fiber to use. In particular, the number of plies to be replaced by glass, and their position within the stacking sequence, must somehow be determined. Because of the expense and time required to fabricate and

test composite panels for structural properties and impact resistance, an analytical or computational tool for predicting hybrid response would be helpful to the design process. In this paper, we describe a relatively new computational model for this analysis, called the *peridynamic* model. We also compare model results against experimental data from ice impact tests.

To simplify the analysis for purposes of illustrating the method and the effect of hybridization, this paper considers only one option for ply-level hybridization, which is to replace fabric plies on both surfaces of a panel with glass fabric plies, resulting in a 20% ply-level hybrid.

2. MATHEMATICAL MODEL

In addition to a variety of practical considerations, application of hybridization to aerospace structural materials has been hindered by the absence of a reliable analytical method that can be used to help assess and optimize hybrid materials under a wide variety of conditions and impact loadings. Computational failure models in wide use within finite element codes, such as the Tsai-Wu (1971) and Hashin (1980) models, are oriented toward initiation of failure in macroscopic coupon tests, and therefore may not be optimal as predictors of local failure and damage propagation during impact. In particular, models of this type may not be totally acceptable methods for modeling fracture nucleation and propagation, particularly involving delamination.

As an alternative to these widely-known methods, the *peridynamic* mathematical model of solid mechanics has been proposed as a technique for modeling damage, fracture, and failure in materials and structures. This method replaces the standard partial differential equations (PDEs) of solid mechanics with integro-differential equations (IDEs). The primary motivation is that the PDEs cannot be applied directly on cracks or other discontinuities, because the required spatial derivatives of the deformation are not defined on these surfaces. In contrast, the IDEs of the peridynamic model remain equally valid regardless of whether any discontinuities are present.

Nearly all computational methods for fracture in general use today apply some set of special equations to the growth of cracks. These equations generally employ concepts from linear elastic fracture mechanics such as the stress intensity factor. Typically, these concepts are most valid when applied to highly idealized situations, such as a single, straight mode-I crack in a homogeneous, two-dimensional solid under quasi-static loading. In real world applications, however, evolution of damage and failure may be far different from these idealized problems. For example, a material may accumulate damage locally near a stress concentration. The nature of the damage at the microstructural level may be nonhomogeneous and strongly influenced by random defects that may or may not be observable by testing methods. At some time during loading, this damage may change from continuous to discontinuous, causing a propagating crack. The deformed and damaged zone near the tip of an advancing crack may be much larger in size than the small process zone that is typically assumed in linear elastic fracture mechanics.

The peridynamic model, because it applies the same fundamental equations to all points in a structure regardless of the presence of damage or cracking, appears to provide a more general and convenient method for the modeling of impact damage and structural failure than standard approaches. These potential advantages are particular desirable for composites, in which the complexity of the microstructure, as well as the presence of multiple length scales, may limit the applicability of standard fracture mechanics concepts.

In a peridynamic body, points in the continuum interact directly with each other across a finite distance. The force interaction between a pair of particles $\mathbf{x}$ and $\mathbf{x}'$ is given by a function $\mathbf{f}(\mathbf{u}(\mathbf{x}',t)-\mathbf{u}(\mathbf{x},t),\mathbf{x}',\mathbf{x},t)$ that depends on the displacements $\mathbf{u}$ at these points, and on their initial positions. The units of $\mathbf{f}$ are force/volume^2. The sum of the forces exerted by all the points $\mathbf{x}'$ on a given point $\mathbf{x}$ provides the net force density at $\mathbf{x}$, which gives the rate of change of momentum:

$$\rho(\mathbf{x})\ddot{\mathbf{u}}(\mathbf{x},t)=\int_{\mathcal{H}}\mathbf{f}(\mathbf{u}(\mathbf{x}',t)-\mathbf{u}(\mathbf{x},t),\mathbf{x}',\mathbf{x},t)\,dV_{\mathbf{x}}+\mathbf{b}(\mathbf{x},t) \qquad (1)$$

where ρ is the mass density and $\mathbf{b}$ is the body force density. Equation (1) is the peridynamic equation of motion. The subregion $\mathcal{H}$ contains all the points in the body that $\mathbf{x}$ interacts with. It is convenient, although not essential, to assume that points separated by a distance greater than some prescribed distance δ, called the *horizon*, do not interact.

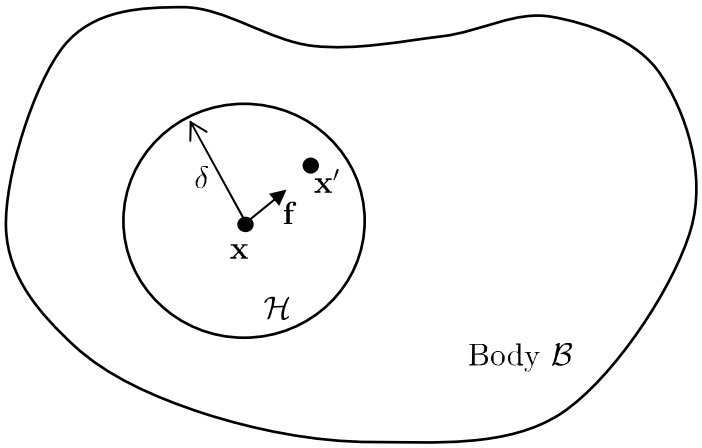

Figure 1. The peridynamic model sums up the forces exerted on any point x through interactions with all neighbors x' within a distance δ.

All constitutive information about the particular material is contained in the function $\mathbf{f}$. Because the direction of $\mathbf{f}$ must be parallel to the relative deformed positions of the points

$\mathbf{x}$ and $\mathbf{x}'$ (due to the fundamental requirement for balance of angular momentum), a constitutive model consists of the relation between $|\mathbf{f}|$ and the deformation of the bond vector $\mathbf{x}' - \mathbf{x}$. A typical peridynamic constitutive model is shown in Figure 2. In this figure, the horizontal axis is bond strain, defined to be the change in length in the deformed bond divided by its initial length:

$$s = \frac{\left|(\mathbf{u}(\mathbf{x}', t) + \mathbf{x}') - (\mathbf{u}(\mathbf{x}, t) + \mathbf{x})\right|}{\left|\mathbf{x}' - \mathbf{x}\right|}$$

The figure also illustrates how damage is introduced into the mathematical model. Bonds break irreversibly when they are strained beyond some predetermined value s_0. After a bond breaks, it no longer sustains any force.

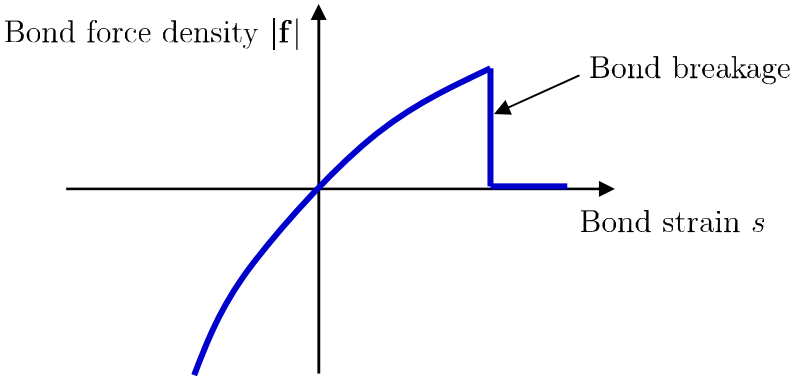

Figure 2. Typical peridynamic constitutive model including damage due to bond breakage.

The simplest peridynamic material model is called *microelastic*. This model assumes that the curve of bond force versus bond strain in Figure 2 is linear prior to bond breakage. The slope of the line, called the *spring constant*, is denoted by c. The spring constant is fitted to the bulk elastic properties of the material. The critical strain for bond breakage, s_0, can be obtained from the measured critical energy release rate G in the case of an ideal crack in a brittle material. The relation between s_0 and G comes from the energy balance for an advancing crack: the work required to break all the bonds that initially connected the material on either side of the crack, per unit crack area, must equal G.

Anisotropy is introduced by allowing bonds in different directions to have different stiffness and failure properties. In the peridynamic model of a fiber-reinforced lamina, the bonds in the direction of the fibers represent the fiber properties, while the bonds in all other directions represent the matrix properties. The fiber bonds and matrix bonds have properties that are independent of each other, including both elastic response and failure

properties. The matrix bonds do not represent the bulk properties of neat resin, since they also include the effects of fiber-resin interfaces and the transverse properties of the fibers.

The peridynamic model of a lamina is illustrated in Figure 3. The spring constants for matrix and fiber bonds are shown as c^{m} and c^{f} respectively. The critical strains for bond breakage in tension are s_0^{mt} and s_0^{ft} for matrix and fiber bonds, respectively. In compression, the matrix and fiber bonds are assumed to fail and the same critical strain, denoted s_0^{c}. This assumption is made because the microbuckling mechanism for lamina failure in compression involves simultaneous localization in both the resin and fibers, hence it is not possible to identify separate failure criteria for each in compression.

The basic test data needed to obtain the parameters in the model are summarized in Table 1. For some parameters, these parameters need to be modified to match data on impact damage.

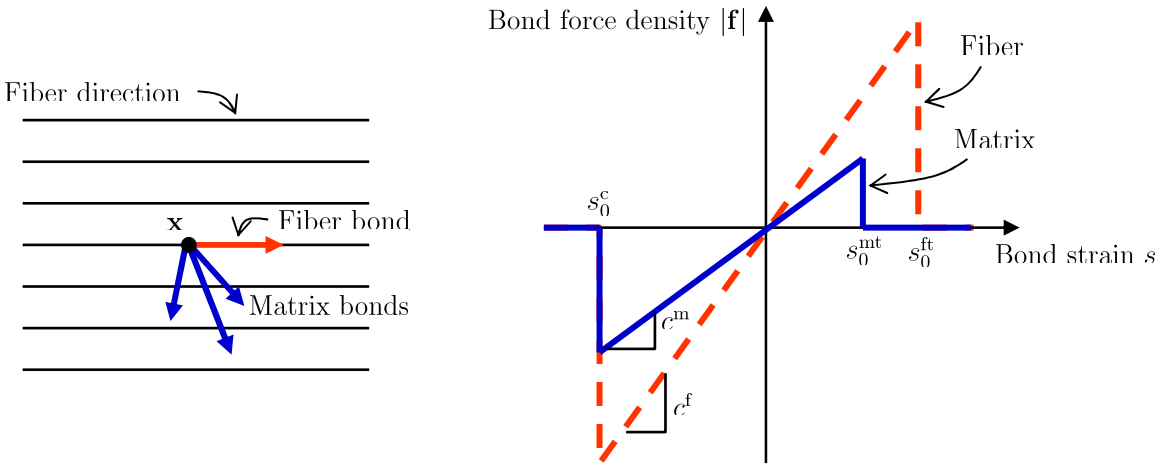

Figure 3. Peridynamic material model for a unidirectional composite has separate properties for fiber bonds and matrix bonds.

Table 1. Material properties used in the peridynamic model for a composite.

Parameter	*Meaning*	*Test data needed*
c^{m}	Spring constant, matrix	Elastic modulus E_{22}
c^{f}	Spring constant, fiber	Elastic modulus E_{11}
c^{i}	Spring constant, interlayer	Elastic modulus E_{33}
s_0^{mt}	Tensile bond breakage strain, matrix	Tensile failure strain ε_2^t
s_0^{ft}	Tensile bond breakage strain, fiber	Tensile failure strain ε_1^t
s_0^{it}	Tensile bond breakage strain, interlayer	Mode-I energy release rate G_{Ic}
s_0^{c}	Compressive bond breakage strain, matrix and fiber	Compressive failure strain ε_1^c
α	Spring constant, shear bonds	Shear modulus μ_{13}
γ_0	Shear angle for shear bond breakage	Mode-II energy release rate G_{IIc}

A fabric lamina is modeled using the same approach, but with two special directions for fiber bonds instead of one. The spring constant in each of the two fiber directions is reduced to one half what it would be in a unidirectional lamina.

A model of a laminate is constructed from a stack of lamina models, each with a particular fiber direction. The laminas interact with each other through peridynamic bonds. Because of the small distances between the layers in a typical laminate, the simple springlike bonds described above do not accurately reproduce the elastic response of the laminate to interlayer shear. To provide a better representation of this mode of deformation, special peridynamic bonds that respond to changes in shear angle, rather than elongation, are used. These *shear bonds* are illustrated in Figure 4. As shown in the figure, the shear angle near a point $\mathbf{x}$ is found from the displaced position of $\mathbf{x}$ and of the nearest point on the adjacent ply, shown as $\mathbf{x} + h\mathbf{n}$, where h is the distance between plies and $\mathbf{n}$ is the unit normal vector. From the equation in the inset, the force applied at $\mathbf{x}$ is directed toward the point at the other end of the shear bond $\mathbf{x}'$, and is proportional to the mean of the shear angles at these two points. The constant of proportionality α is fitted to the interlayer shear modulus. Shear bonds can break irreversibility in the shear angle exceeds a critical value γ_0 that is fitted to the energy release rate in Mode II, which can be measured in and end-notch-flexure (ENF) test. Shear bond breakage does not occur in the model until in-ply bonds, either matrix or fiber bonds, have broken in one of the adjacent plies due to either tension or compression. Therefore, in-ply damage is required to nucleate delaminations.

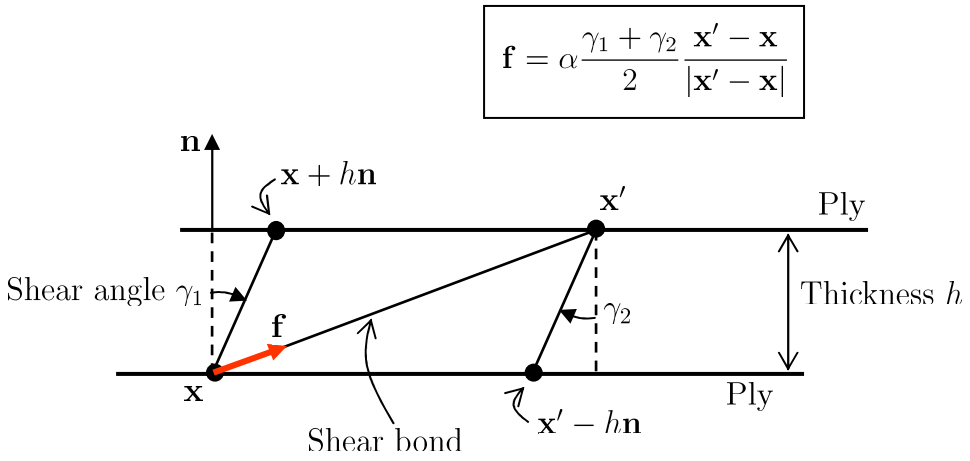

Figure 4. Schematic of peridynamic bonds used to connect plies in a laminate.

The computer code that implements the peridynamic continuum theory is called EMU (Silling and Askari, 2005). This is a three-dimensional, meshless, Lagrangian code. The numerical method consists of a spatial discretization in which the integral in the peridynamic equation of motion, Equation (1), is replaced by a finite sum. Time integration is performed using a standard explicit central differencing method.

3. EXAMPLE PROBLEMS AND TEST DATA

This section describes model results and impact testing for simulated hail balls striking baseline and 20% glass hybrid composite laminates. The baseline material is a toughened-epoxy, intermediate-modulus, carbon-fiber composite.

Ground hail against thin panels

In this problem, a simulated hail ball with mass 0.0996kg and diameter 0.06m strikes a composite panel. Two impact energies are considered: 136J and 90J. The panel is a rectangle with dimensions 0.254m x 0.356m. The geometry is shown in Figure 5. A boundary region with thickness 0.006m around the edges of the panel is modeled as loosely clamped, meaning that the out-of-plane displacement is set to zero, while the in-plane displacements are not constrained.

The panel is quasi-isotropic graphite-epoxy laminate with 8 tape plies. One additional fabric ply is included on each face of the panel. In the baseline material, the fabric is graphite-epoxy. In the hybrid material, the fabric in both the top and bottom layers is replaced by S-2 glass. Since 2 of the 10 plies are replaced, the result is a 20% glass

hybrid. The total thickness of the panel is 1.9mm, which is not changed by the hybridization. Table 2 shows the values of parameters used in the computational model.

Figure 6 shows the deflected baseline panel at the time of maximum force exerted on the projectile. As shown in the contours of tensile strain, matrix bonds in the rear ply have exceeded their breakage strain, which is 0.014. This creates in-ply damage in the rear ply that nucleates delaminations as shown in the figure. The bending strains are slightly larger in the hybrid panel (not shown) because of the reduced stiffness of the glass fabric. However, this increase in strain is not enough to exceed the breakage strain in the glass ply, which is 0.028. Therefore, in the hybrid, in-ply damage does not occur until the second-to-last ply, which is graphite tape, exceeds its breakage strain.

As shown in Figure 7, the calculated delaminated area reflects the trend seen in the ultrasonic measurements. At a nominal impact energy of 136 J, the hybrid shows a modest reduction in damaged area. According to the model, the reduction is primarily due to the larger value of s_0^{mt} in the glass fabric, which is the breakage strain for matrix bonds. This more than offsets the increase in tensile bending strain sustained in the bottom ply due to decreased stiffness in the glass fabric. Because of the larger tensile breakage strain, no in-ply damage occurs in the glass fabric. (Fiber breakage does not occur in this problem.) The delaminations that occur in the hybrid are nucleated by the second-to-last ply, which is a graphite tape layer.

For the same reason, as impact energy is increased from zero, the onset of delamination is delayed in the hybrid. The delaminations do not nucleate in the hybrid material until the second-to-last ply sustains a large enough bending strain to cause in-ply damage. In contrast, in the baseline laminate, delaminations nucleate when the last layer, which is graphite fabric, reaches its breakage strain. This higher threshold energy for delamination is illustrated in Figure 8, which shows model results for delaminated area with an impact energy of 90 J. This value is just above the energy required to nucleate damage in the hybrid, as indicated by the small delaminated area.

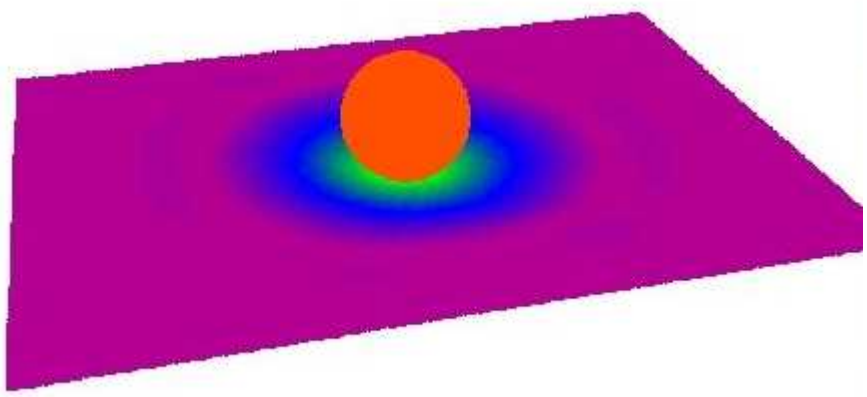

Figure 5. Computational model of the panel and ice ball. Colors indicate displacement.

Table 2. Material parameters used in the example problems.

Parameter	*Graphite-epoxy fabric*	*Glass-epoxy fabric*	*Graphite-epoxy tape*
E_{11}	71.0 GPa	24.0 GPa	142.0 GPa
E_{22}	71.0 GPa	24.0 GPa	6.9 GPa
E_{33}	6.9 GPa	6.9 GPa	6.9 GPa
$\mu_{13} = \mu_{23}$	2.8 GPa	2.8 GPa	2.8 GPa
s_0^{mt}	0.014	0.028	0.014
s_0^{ft}	0.019	0.038	0.019
s_0^{it}	0.014	0.014	0.014
s_0^{c}	-0.017	-0.034	-0.017
γ_0	0.01	0.01	0.01

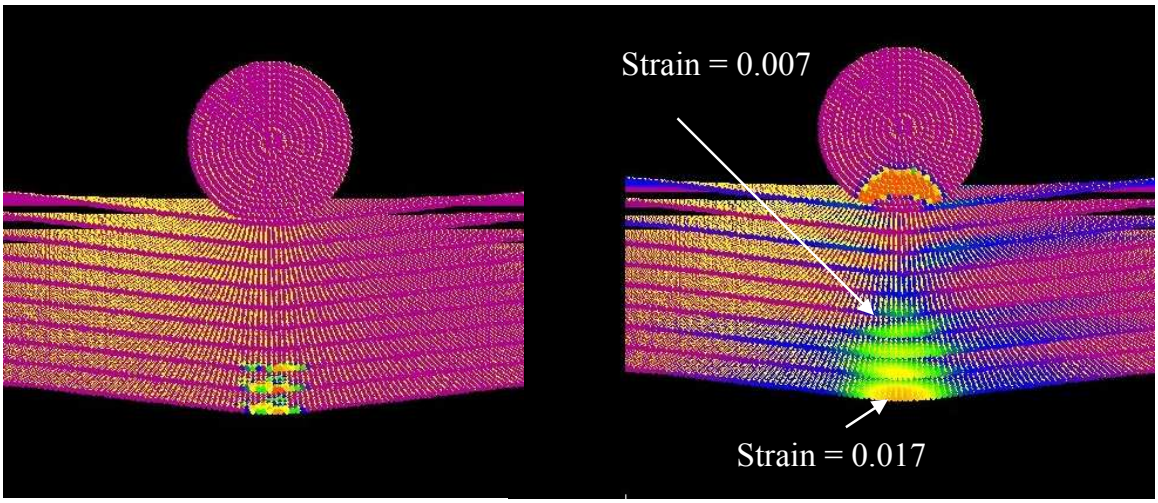

Figure 6. In the baseline panel, delaminations (left) are nucleated by damage due to tensile bond strain in the rear ply (right).

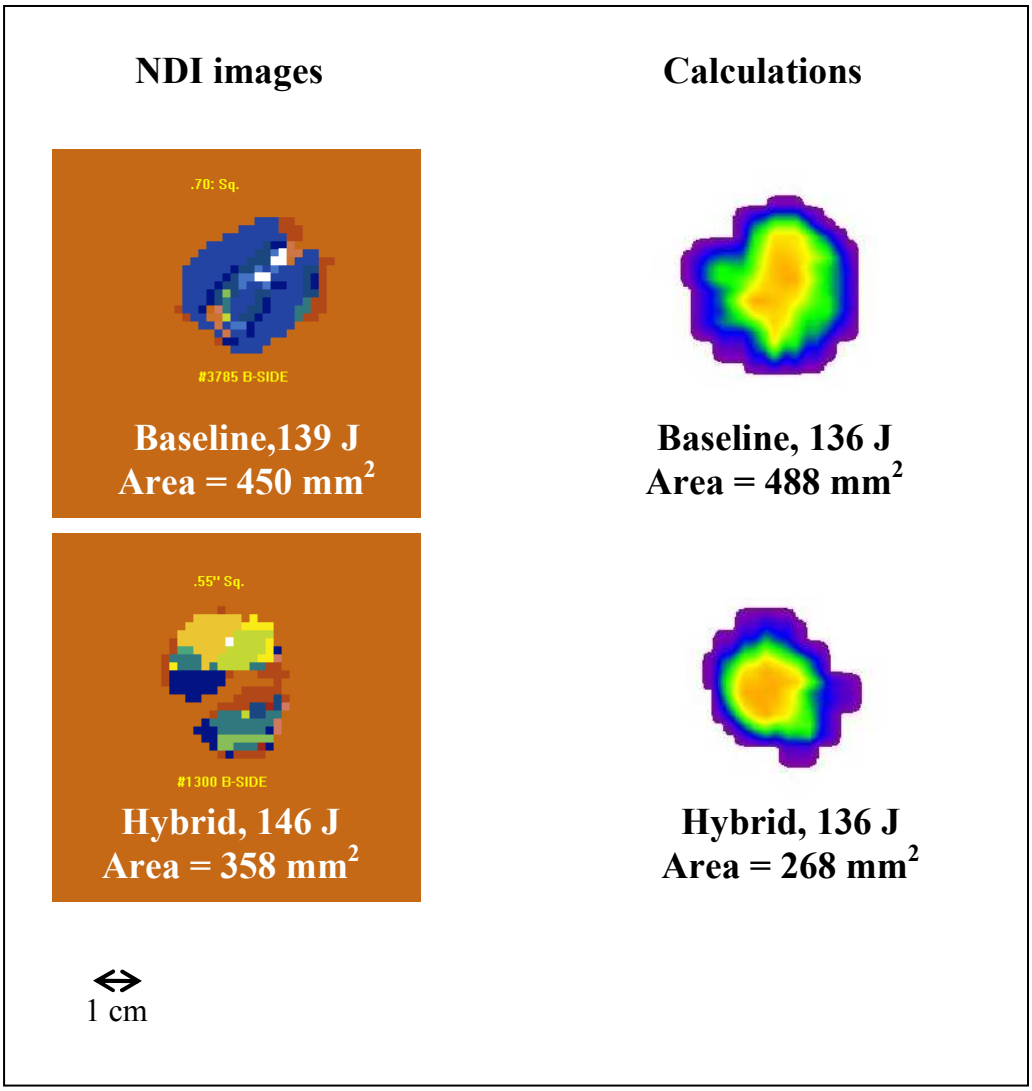

Figure 7. Ultrasonic (NDI) images, damaged area values, and computational results for 10-ply panels impacted by ice balls with energy near 136J, for both baseline and hybrid panels. The length scale is the same for all four images. Hybridization tends to reduce the damaged area.

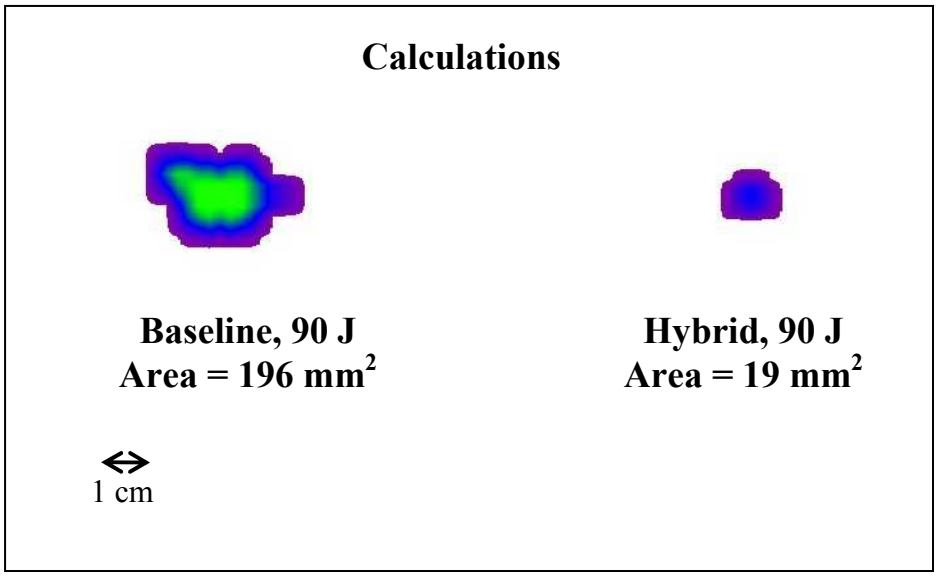

Figure 8. Computational results for delaminated area in 10-ply panels impacted by ice balls with energy 90J. Hybridization increases the threshold energy for creating delamination.

In-flight hail impact on a thick panel

In this problem, the ice ball described in the previous section strikes a 26-ply panel, either the baseline laminate or the 20% glass hybrid. The geometry and boundary conditions on the panel are the same as in the low-velocity case described previously. The material properties are shown in Table 2.

The model predicts extensive delamination in both the baseline and hybrid materials. Significant tearing of the rear layer due to fiber breakage is also present, but is much more pronounced in the baseline material. As shown in Figure 9, the baseline panel becomes perforated, temporarily opening a sufficiently large hole that a small amount of ice gets through. The hole eventually closes again as the panel rebounds. A much smaller amount of ice is predicted to perforate the hybrid panel.

Figure 10 compares the model predictions for tearing in the rear ply after the panel has rebounded. Only the rear lamina is shown. The tearing includes fiber bond breakage, which does not occur in the low-energy impact problems discussed earlier. The length of the tear in the rear ply is about twice as great in the baseline material as in the hybrid. This difference is due to the higher bond breakage strain for fiber bonds in the glass fabric model. The figure also shows photographs of the rear of test panels impacted at

slightly higher impact energy. The trend of lower damage in the hybrid predicted by the model is seen in these photographs.

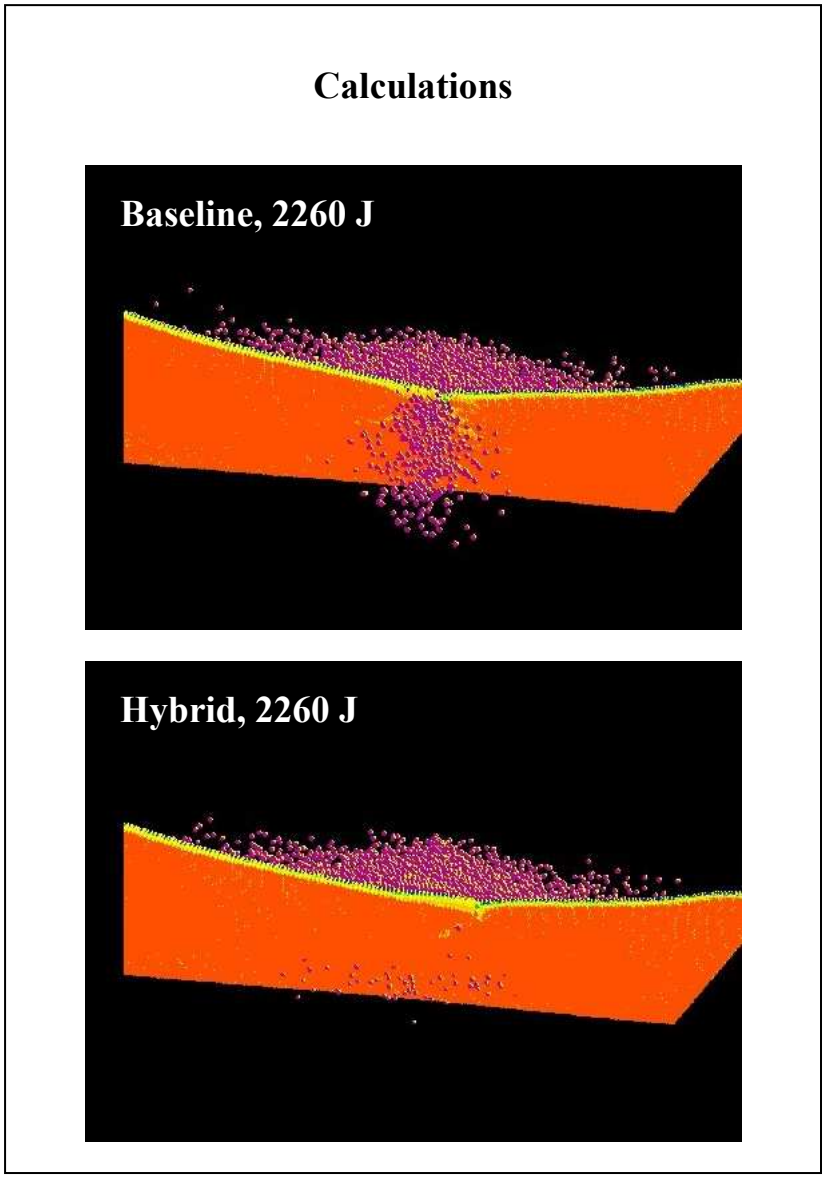

Figure 9. Cross-sectional views of panel and projectile deformation for an ice ball striking thick composite panels with energy 2260 J. The ice ball becomes fragmented. In the case of the baseline panel, a significant number of these fragments are predicted to perforate the panel. Only a small amount of projectile material perforates the hybrid.

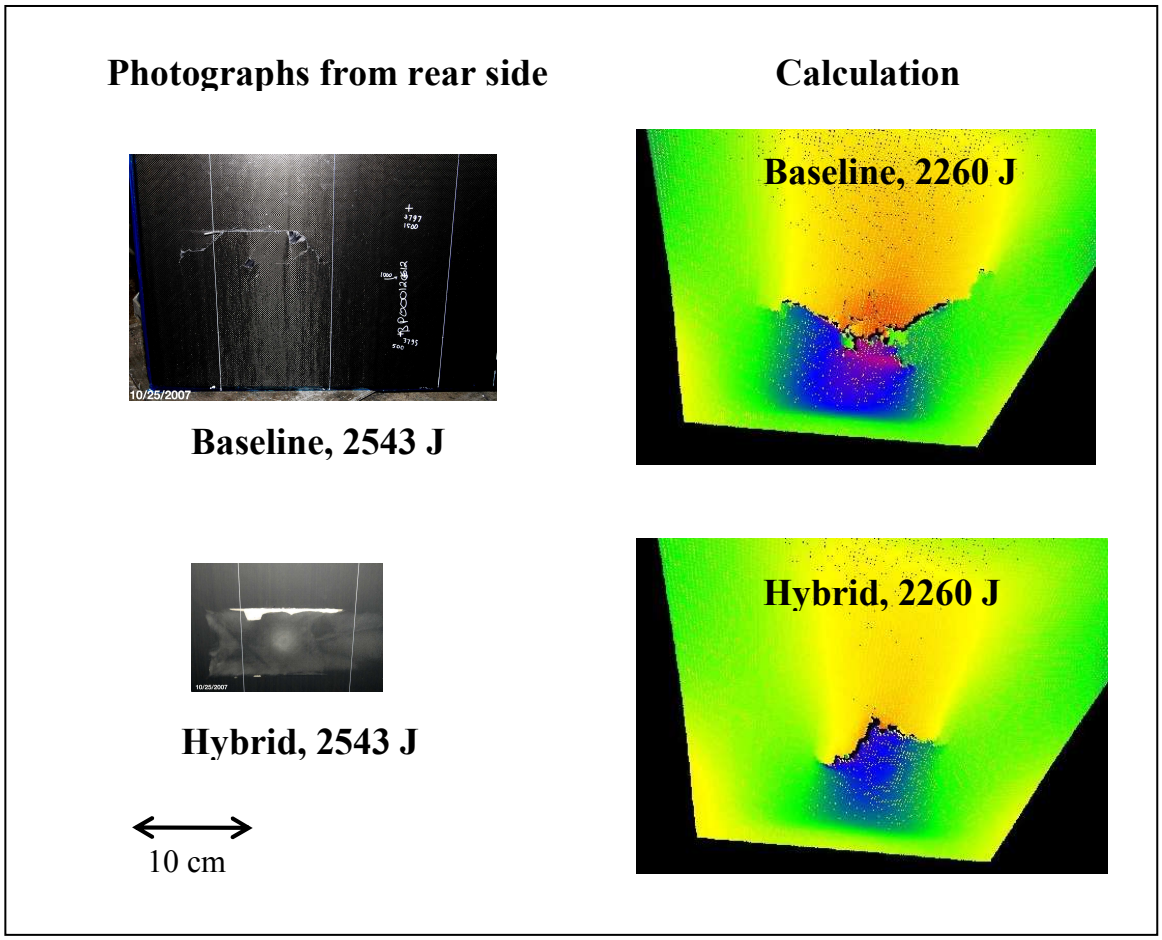

Figure 10. Computational predictions for tearing of the rear lamina for the baseline and hybrid panels struck by ice at 2260J. At the left, photographs of test panels at comparable impact energy.

4. CONCLUSIONS

The method of analysis presented here appears to hold promise for the evaluation of alternative hybrid layups under various types of impact loading, including differences in impact energy, velocity, deformability of the projectile, panel size, and different boundary conditions. The method appears to reproduce the primary modes of damage and failure in laminates under impact loading, including tearing, fracture, and perforation. One observation that appears to be clear from experience with the model is that the deformation of the projectile must be included in any realistic model of ice impact, since this strongly affects the contact area, particularly at high impact energies.

The examples shown suggest that the difference in response between baseline and hybrid materials with respect to impact damage by ice can be understood by a relatively simple mechanism. The glass fabric has higher tensile failure strain than the graphite fabric. This delays the onset of damage within plies due to tensile bending strain near the rear of the panels. This delay in the appearance of in-ply damage, which is assumed to nucleate delaminations, is responsible for the lower delaminated area in the hybrid in the low-energy impacts. In the high-energy impacts, the greater tensile strain to failure in the glass fabric is also responsible for the reduced gross damage at the rear of the panel and hence greater resistance to perforation.

Although compressive failure is not significantly involved in the problems shown in this paper, they would be expected to have a greater role for different kinds of projectiles. For example, a small-radius rigid impactor would tend to induce greater compressive strains near the top layers of the laminate than a large-radius deformable projectile like an ice ball. Different projectiles and other sources of damage would need to be evaluated both computationally and through testing before reaching any general conclusions about possible advantages of hybrid materials.

ACKNOWLEDGMENT

Sandia is a multiprogram laboratory operated by Sandia Corporation, a Lockheed Martin Company, for the United States Department of Energy's National Nuclear Security Administration under contract DE-AC04-94AL85000.

REFERENCES

D. F. Adams and A. K. Miller (1975), An analysis of the impact behavior of hybrid composite materials (graphite/epoxy laminate with glass and nylon fibers), *Materials Science and Engineering*, Vol. 19, pp. 245-260.

E. Askari, J. Xu, and S. A. Silling (2006), Peridynamic analysis of damage and failure in composites, AIAA-2006-88, 44th AIAA Aerospace Sciences Meeting and Exhibit, Reno, Nevada, Jan. 9-12, 2006.

P. W. R. Beaumont, P. G. Riewald, and C. Zweben (1975), Methods for improving the impact resistance of composite materials, in *Foreign object impact damage to composites*, ASTM special publication, pp. 134-158.

G. Dorey, G. R. Sidey, and J. Hutchings (1978), Impact properties of carbon fibre/Kevlar 49 fibre hybrid composites, *Composites*, Vol. 9, pp. 25-32.

Z. Hashin (1980), Failure criteria for unidirectional fiber composites, *Journal of Applied Mechanics*, Vol. 47, pp. 329-334.

Y.-S. Lee, K.-H. Kang and O. Park (1997), Response of hybrid laminated composite plates under low-velocity impact, Computers and Structures, Vol. 65, pp. 965-974.

N. K. Naik, R. Ramasimha, H. Arya, S. V. Prabhu and N. S. Rao (2001), Impact response and damage tolerance characteristics of glass–carbon/epoxy hybrid composite plates, *Composites Part B: Engineering*, Vol. 32, pp. 565-574.

R. Park and J. Jang (2001), Impact behavior of aramid fiber/glass fiber hybrid composite: Evaluation of four-layer hybrid composites, Journal of Materials Science, Vol. 36, pp. 2359-2367.

S. A. Silling (2000), Reformulation of elasticity theory for discontinuities and long-range forces, *Journal of the Mechanics and Physics of Solids*, Vol. 48, pp. 175-209.

S. A. Silling and E. Askari (2005), A meshfree method based on the peridynamic model of solid mechanics, *Computers and Structures*, Vol. 83, pp. 1526-1535.

S. W. Tsai and E. M. Wu (1971), A general theory of strength for anisotropic materials, *Journal of Composite Materials*, Vol. 5, pp. 58-80.